

Enantiomerically Pure Poly(oxymethylene) Helices: Correlating Helicity with Centrochirality

by Simon Eppacher^a), Gerald Giester^b), Jan W. Bats^c), and Christian R. Noe^{*a})

^a) Department of Medicinal Chemistry, University of Vienna, Althanstrasse 14, A-1090 Wien
(phone: +43 1 4277 55103; fax +43 1 4277 9551; e-mail: christian.noe@univie.ac.at)

^b) Department of Mineralogy and Crystallography, University of Vienna, Althanstrasse 14, A-1090 Wien

^c) Department of Organic Chemistry, University of Frankfurt, Max-von-Laue-Strasse 7, D-60438
Frankfurt am Main

A first series of enantiomerically pure helical oligo(formaldehyde)s (= oligo(oxymethylen)s) **16–20** was synthesized. To induce the chiral uniformity of the helices, we used (1*S*)-2,2-dimethyl-1-phenylpropan-1-ol (**14**) to generate the end groups at the α and ω terminus (*Scheme 6*). Propanol **14** was accessible from its racemate by acetal formation with lactol **12** and separation of the diastereoisomers (*Scheme 5*). The helicity of the oligomers was investigated by temperature-dependent CD, NMR, and optical-rotation studies. In addition to qualitative considerations concerning the helicity of oligo(formaldehyde)s, we performed calculations of the dimer **17** and the pentamer **20** as well as X-ray structure analyses of the dimer **17** and the tetramer **19** to establish the handedness of the helices and to correlate their sense with the absolute configuration of the inducing stereogenic center. The results may be of relevance with respect to induction and propagation of chirality in prebiotic chemistry.

Introduction. – Formaldehyde is one of the ‘most fundamental organic molecules’. It is also a versatile building block in organic chemistry and found in several modifications. In the gas phase, it exists as monomeric formaldehyde, in aqueous solution, it forms a hydrate (formalin, formol), and in the solid state, it is composed of either cyclic trimers (1,3,5-trioxane, metaformaldehyde), cyclic tetramers (1,3,5,7-tetroxocane), or linear poly(oxymethylene) (paraformaldehyde), respectively [1–3]. Short oligomers of poly(oxymethylene) were found in the tail of the *Halley* comet [4]. It is well accepted that paraformaldehyde forms a helix as it was shown by theoretical calculations [5], by IR spectroscopy [6], and by X-ray analysis [7–13] (see below). During our investigation of stereoelectronic effects, we became interested in the structure of oligomers of formaldehyde, *i.e.*, of 1,13-diphenyl-2,4,6,8,10,12-hexaoxa-tridecane [14] and its corresponding heptamer (= 1,17-diphenyl-2,4,6,8,10,12,14,16-octaaoxaheptadecane) [15], respectively. These oligomers crystallize as helices and may serve as ‘most basic reference’ for the investigation of stereoelectronic effects, the anomeric effect (interaction of the n_0 lone pair of the O-atom and the σ^* orbital of the C–O bond), in particular, since there are no other interacting effects [16].

To synthesize for the first time an enantiomerically pure oligo(formaldehyde) (= oligo(oxymethylene)) helix with predicted handedness, we decided to use a chiral alcohol, (1*S*)-2,2-dimethyl-1-phenylpropan-1-ol (**14**), to generate both end groups (at the α and ω terminus) of the formaldehyde oligomer. We report the synthesis and

characterization of a first series of enantiomerically pure oligo(oxymethylene)s up to pentamer **20**, capped by **14**. As evidence of the correct structure, we additionally present the crystal structure of the dimer **17** and the tetramer **19**.

Results and Discussion. – 1. *Qualitative Considerations of the Helicity of Poly(formaldehyde)*. The conformational analysis of the poly(formaldehyde) helix is in line with the rules applied by *Eschenmoser* and *Dobler* for the conformational analysis of homo-DNA [17] and p-RNA and which is also comprehensively discussed in the book of *Quinkert, Egert, and Griesinger* [18].

If only the three idealized staggered conformations (+*sc*, –*sc*, and *trans*) are considered, one needs two criteria to explain the helicity of poly(formaldehyde): *a*) the anomeric effect (stereoelectronic rule), *b*) each electron pair should be involved in one anomeric effect. This is the generalized b(ulky), pl(anar), and H rule (b-pl-H rule) [19] with one additional H instead of the b(ulky) group. Depending on whether one starts from position *a*) or *b*) depicted in *Fig. 1*, one ends up with a right- or a left-handed helix, respectively. Since benzyl alcohol, which was first used for the end groups at the α and ω terminus, is an achiral substrate, there is no preference to start from position *a*) or *b*), and as a result, a racemic mixture of oligomers is formed [14][15]. To obtain a first enantiomerically pure oligo(formaldehyde), we decided to use a chiral alcohol to generate the end groups. By applying the b-pl-H rule [19], it can be predicted that helix formation will be left-handed if both end groups will be derived from a ‘*B*’-configured alcohol, and a right-handed helix will be formed if both end groups will be an ‘*A*’-configured alcohol.

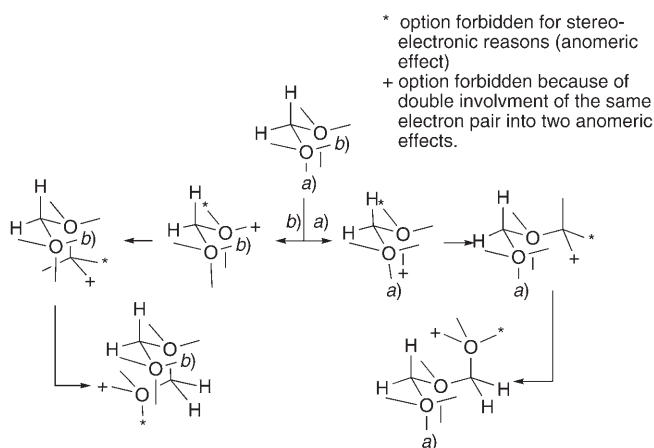
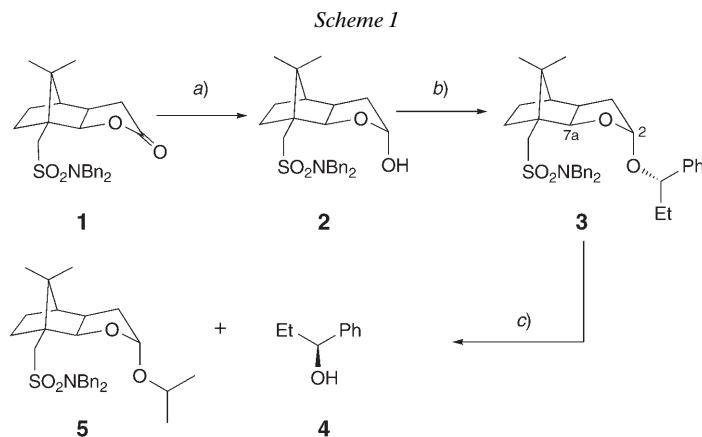


Fig. 1. *Qualitative conformational analysis of an oligo(oxymethylene) strand*

2. *Synthesis of the Protected Enantiomerically Pure Oligo(oxymethylene)s*. As a first enantiomerically pure inducer for the oligomerization, we prepared (1*S*)-1-phenylpropan-1-ol (**4**), a ‘*B*’-type compound, from lactone **1** in three steps (*Scheme 1*). We used lactol **2** [20][21], which is accessible from lactone **1** by reduction with diisobutylaluminium hydride (DIBAL) in 90% yield, to resolve (\pm)-**4**. Acetal **3** was

obtained with a diastereoselectivity of 4.5 : 1 by reacting lactol **2** with an excess of (\pm)-**4** in the presence of catalytic amounts of triphenylphosphonium bromide. The good diastereoselectivity can be explained by a combination of anomeric, *exo*-anomeric, and steric effects as described earlier [22–26] and will be discussed in detail in a forthcoming publication. The diastereoisomer of acetal **3**, formed in minor quantities, could be removed by flash chromatography. The enantiomerically pure (1*S*)-1-phenylpropan-1-ol (**4**) was liberated by treatment of acetal **3** with catalytic amounts of TsOH in ³PrOH/CH₂Cl₂. Propanol **4** could be separated from acetal **5** by bulb-to-bulb distillation.



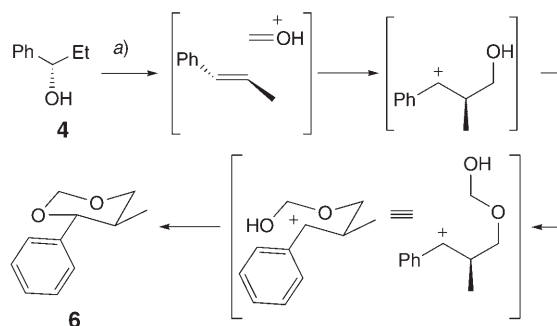
a) DIBAL, toluene; 90%. b) (\pm)-**4**, cat. [HPPh₃]Br, CH₂Cl₂; 49% of **3** and 31% of **3**/diastereoisomer of **3**. c) TsOH, ³PrOH/CH₂Cl₂ 3 : 1; 47%.

Unfortunately, a trial experiment with racemic (\pm)-**4**, which we carried out to investigate the oligomerization reaction under the same conditions as in the case of benzyl alcohol (*Scheme 2*), had an unexpected outcome. Instead of the expected oligomerization products, we found *trans*-5-methyl-4-phenyl-1,3-dioxolane (**6**). For its formation, we propose the following reaction sequence: elimination of H₂O from 1-phenylpropan-1-ol, a *Prins* reaction, and a final cyclization with a second molecule of formaldehyde [27].

To prevent the elimination reaction leading to the *Prins* reaction sequence, we chose a 4-nitrophenyl group to destabilize the positive charge at the benzylic position, which is generated in the elimination step. The 1-(4-nitrophenyl)ethanol (**8**) was obtained by reduction of 4-nitroacetophenone (**7**) with NaBH₄ in EtOH and was treated under our standard oligomerization conditions (*Scheme 3*). As foreseen, the elimination reaction was now suppressed and did no longer control the scene. However, instead of the wanted longer oligomers we could only isolate the monomer **9** in reasonable yields.

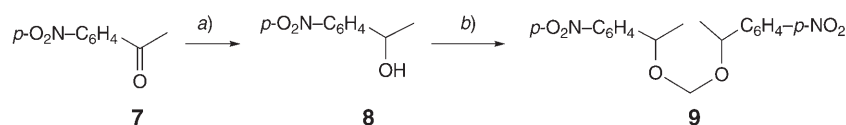
As the next b-pl-H-type chiral inducer, we tested lactol **2** (*Scheme 4*). But, as in the case of (\pm)-**4**, we obtained the dioxolane derivative **10**, which is probably built by the same elimination, *Prins* reaction, and cyclization sequence as that leading to dioxolane **6**.

Scheme 2



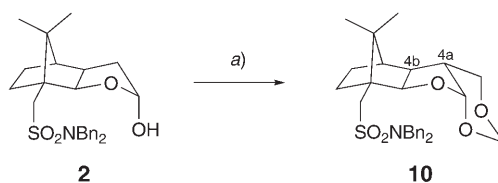
a) Cat. H_2SO_4 , paraformaldehyde, benzene; 81%.

Scheme 3



a) NaBH_4 , EtOH; 98%. b) Cat. H_2SO_4 , paraformaldehyde, benzene; 83%.

Scheme 4

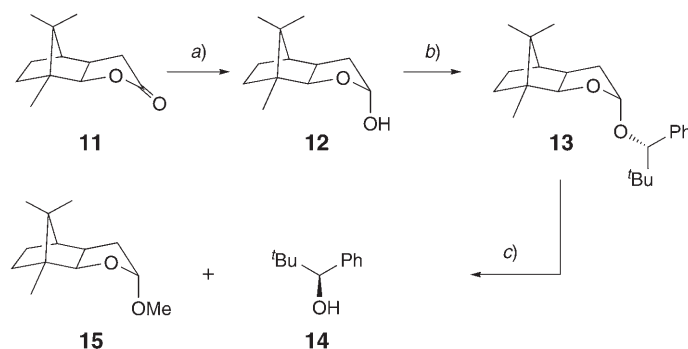


a) Cat. H_2SO_4 , paraformaldehyde, benzene; 37%.

Finally, we decided to use (1*S*)-2,2-dimethyl-1-phenylpropan-1-ol (**14**) as chirality-inducing unit (Scheme 5). To separate racemic **14**, we used lactol **12**, which is accessible from lactone **11** by reduction with DIBAL. By using a fourfold excess of (\pm)-**14**, we obtained acetal **13** with the good diastereoselectivity ratio of 5.4:1, which could be enriched to a 12:1 ratio and to pure **13**, depending on the conditions used for flash chromatography. When lactol **2** was used instead of lactol **12**, the corresponding acetal was not separable from the excess of (\pm)-**14**. The enantiomerically enriched **14** was released by treatment of acetal **13** with a catalytic amount of TsOH in MeOH/ CH_2Cl_2 1:1 in 67% yield.

By using first (\pm)-**14** for our standard oligomerization protocol (2 h in refluxing benzene with catalytic amounts of H_2SO_4), we found a complex reaction mixture. By optimizing the reaction conditions, we realized that the reaction was complete within 5 min in refluxing benzene/cat. H_2SO_4 and an excess of paraformaldehyde (Scheme 6).

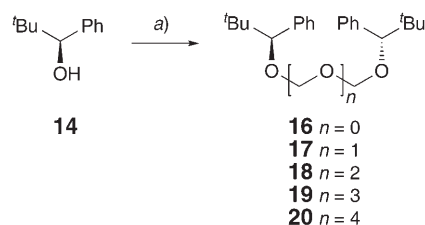
Scheme 5



a) DIBAL, toluene; 91%. b) (±)-**14**, cat. [HPPPh₃]Br, CH₂Cl₂; 38% of **13**, and 49% of **13**/diastereoisomer of **13**. c) TsOH, MeOH/CH₂Cl₂ 1:1, 67%.

By immediate quenching of the reaction with NaHCO₃, we could isolate our desired oligomers up to a pentamer **20** in yields which were sufficient for most characterizations.

Scheme 6



a) Cat. H₂SO₄, paraformaldehyde, benzene; 12% (**16**), 18% (**17**), 8% (**18**), 8% (**19**), and 1% (**20**).

3. *Characterization of the Compounds.* In the ¹H-NMR spectrum of compound **3**, H–C(2) is shifted downfield by 0.33 ppm compared to the corresponding signal in the diastereoisomer of **3**, and H–C(7a) of **3** is shifted upfield by 0.15 ppm compared to H–C(7a) of the diastereoisomer of **3**. As discussed in an earlier paper [28], this indicates the (*S*)-configuration at C(1) of the 1-phenylpropoxy part of acetal **3**, which was established by the optical rotation of the liberated alcohol **4**.

The structure of the dioxolane derivative **10** was established by its ¹H- and ¹³C-NMR, HSQC, HMBC, COSY, and NOESY data. The relative configuration at H–C(4a) of **10** was ascertained by a cross-peak of the signal of one Me group with the signal of H–C(4a).

As in the case of acetal **3**, the signal of H–C(2) of **13** is shifted downfield by 0.30 ppm compared to that of its diastereoisomer, and H–C(7a) of **13** is shifted upfield by 0.65 ppm compared to H–C(7a) of its diastereoisomer. Again, this shows the (*S*)-configuration at C(1) in the 2,2-dimethyl-1-phenylpropoxy part of acetal **13**, which was again established by the optical rotation of the liberated alcohol **14** [29].

Since the oligomers **16–20** all possess a twofold axis of symmetry, we observed only one set of signals in the NMR spectra. For the monomer **16**, we found a *s* at $\delta(\text{H})$ 4.41 due to the OCH_2O group and a *s* at $\delta(\text{H})$ 4.36 due to $\text{H}-\text{C}(1,5)^1$. For the dimer **17**, however, we found two *ds* at $\delta(\text{H})$ 4.96 and 4.36 which are due to the two diastereotopic H-atoms of the OCH_2O groups. The $\Delta\delta$ value can be explained by the fact that one of the two H-atoms of the OCH_2O groups is in close contact to the Ph group and therefore shielded, whereas the other one is too far-off from the Ph group to be influenced. The comparably small J_{gem} value of 7.1 Hz is typical for normal formaldehyde acetals. In the ^{13}C -NMR spectrum of **17**, we found (as expected) one *t* at $\delta(\text{C})$ 88.3 due to the two equivalent OCH_2O groups. For the trimer **18**, we found, according to HSQC and HMBC, a *s* at $\delta(\text{H})$ 4.88 that is correlated to the inner OCH_2O group ($\text{CH}_2(5)^1$) and two *ds* for the outer OCH_2O groups ($\text{H}_a-\text{C}(3)$, $\text{H}_a-\text{C}(7)$ and $\text{H}_b-\text{C}(3)$, $\text{H}_b-\text{C}(7)$, resp.) at $\delta(\text{H})$ 4.78 and 4.37, respectively. This shift difference of the two pairs of H-atoms can be explained as in the case of dimer **17**, and also $J_{\text{gem}} = 7.0$ Hz is almost the same as for **17**. In the ^{13}C -NMR spectrum of **18**, the inner C(5) gives rise to a *t* at $\delta(\text{C})$ 87.4, while the outer two C-atom signals (C(3) and C(7)) appear as one *t* at $\delta(\text{C})$ 89.0 which was again verified by HSQC and HMBC data. As expected, we observed a *ca.* 1:2 intensity ratio of the two *ts*, in accord with a C_2 symmetry. For the tetramer **19**, we found, in addition to the coupling of the outer diastereotopic H-atoms ($\text{H}_a-\text{C}(3)$, $\text{H}_a-\text{C}(9)$ and $\text{H}_b-\text{C}(3)$, $\text{H}_b-\text{C}(9)$, resp.¹⁾) at $\delta(\text{H})$ 4.73 and 4.37, a coupling of the inner H-atoms of the OCH_2O groups ($\text{H}_a-\text{C}(5)$, $\text{H}_a-\text{C}(7)$ and $\text{H}_b-\text{C}(5)$, $\text{H}_b-\text{C}(7)$, resp.) at $\delta(\text{H})$ 4.76 and 4.71, as shown again by HSQC and HMBC measurements. In the ^{13}C -NMR spectrum of **19**, the inner two C-atoms (C(5) and C(7)) give rise to one *t* at $\delta(\text{C})$ 88.1, while the outer two C-signals (C(3) and C(9)) resonate as one *t* at $\delta(\text{C})$ 89.5, which was again verified by HSQC and HMBC measurements. For the ^1H -NMR spectrum of the pentamer **20**, we observed three sets of signals for the OCH_2O groups. One *s* corresponding to the innermost OCH_2O group at $\delta(\text{H})$ 4.78, one pair of *ds* for the second-outermost OCH_2O groups ($\text{H}_a-\text{C}(5)$, $\text{H}_a-\text{C}(9)$ and $\text{H}_b-\text{C}(5)$, $\text{H}_b-\text{C}(9)$, resp.¹⁾) appearing at $\delta(\text{H})$ 4.86 and 4.80, and an other pair of *ds* for the outermost OCH_2O groups ($\text{H}_a-\text{C}(3)$, $\text{H}_a-\text{C}(11)$ and $\text{H}_b-\text{C}(3)$, $\text{H}_b-\text{C}(11)$, resp.) showing up at $\delta(\text{H})$ 4.79 and 4.46. Again, the signals were correlated by a combination of HSQC and HMBC measurements. In the ^{13}C -NMR, we observed three *ts* for the corresponding OCH_2O C-atoms. As shown by the HSQC and HMBC plots, C(7) resonates at $\delta(\text{C})$ 88.7, C(3,11) at $\delta(\text{C})$ 89.7, and, finally C(5,9) at $\delta(\text{C})$ 88.3, the three *ts* exhibiting a *ca.* 1:2:2 intensity ratio.

To get additional experimental proof for the helical properties of our oligomers **16–20**, we investigated temperature-depending CD spectra. Unfortunately, we observed only little effects in the oligomers **16–20**, which we also observed for the monomer **14**, the latter being chosen as reference. For example, the pentamer **20** shows (as expected) a 10% decrease of ellipticity at λ_{max} 260 nm when the temperature was increased from 4° to 70°. However, when we examined alcohol **14** as a reference, we also observed a 13% decrease of ellipticity by increasing the temperature from 4° to 70°. Besides these only minor changes in the ellipticity with temperature, it was also found that the

¹⁾ Arbitrary atom numbering of the heterochain (C(1) is Ph-substituted); for systematic names, see *Exper. Part*.

absolute ellipticity of the oligomers was in the same range as that of the reference alcohol **14**. In conclusion, no evidence was found by CD spectroscopy supporting the occurrence of helix formation.

Next, we examined the temperature-dependence of the $^1\text{H-NMR}$ (300 MHz) signals of the three inner OCH_2O units of pentamer **20** in relation to the signals of $\text{H-C}(1,13)^1$ (Fig. 2). As can be seen from Fig. 2, the $\text{H}_a\text{-C}(5,9)$ and $\text{H}_b\text{-C}(5,9)$ signals are shifted upfield by 0.018 and 0.009 ppm, respectively, while the $\text{CH}_2(7)$ signals are shifted downfield by 0.013 ppm, when the temperature was increased from 28° to 88° . In comparison to these changes, the signal of $\text{H-C}(1,13)$ remains within a 0.001 ppm range in this temperature interval. By cooling down the sample to the starting temperature, we obtained the same spectra as at the beginning. This suggests a conformational reversibility within the heating and cooling cycle. These results are a clear indication for an ordered structure in the pentamer **20**, which breaks down as the temperature is raised.

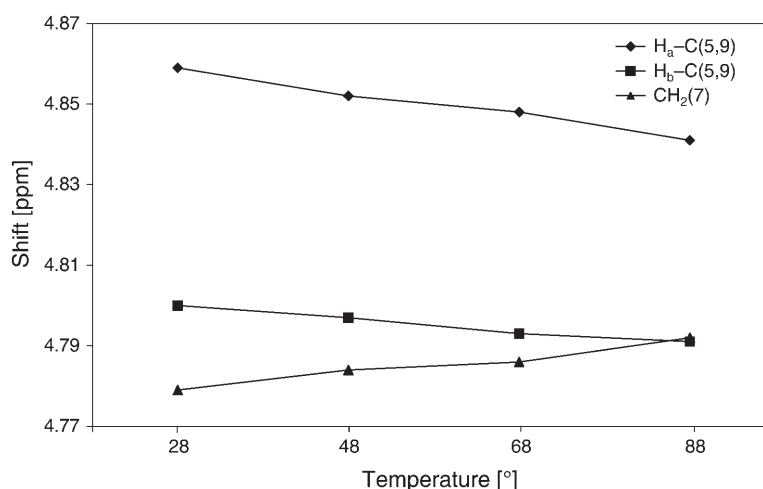


Fig. 2. Temperature dependency of selected $^1\text{H-NMR}$ signals of pentamer **20**

As a next criterion for the structure attribution of our oligomers, we examined the temperature dependency k of the optical rotation of the oligomers **16–20** at 589 and 436 nm. In contrast to the temperature-dependent CD spectra, we observed a clear difference of the temperature dependency k of the optical rotation of the oligomers **16–20**, in contrast to the monomer **14** (Fig. 3), which was measured at 589 nm. For example, the pentamer **20** ($n = 4$) shows the largest dependency of the optical rotation with temperature ($k([\alpha]_D) = 1.41/^\circ$), while the reference alcohol **14** exhibits a far smaller ($[\alpha]_D$) value $k(0.06/^\circ)$. All oligomers and the reference alcohol **14** show a linear dependency of the specific optical rotation within the measured temperature range ($20\text{--}50^\circ$), with a linearity coefficient larger than 0.99.

In addition to this fact, also the absolute specific rotation varies significantly on increasing the chain length (Fig. 4): We observed a large increase of $[\alpha]_D$ for the monomer **16** ($n = 0$) compared to the small value for the reference alcohol **14**, and a

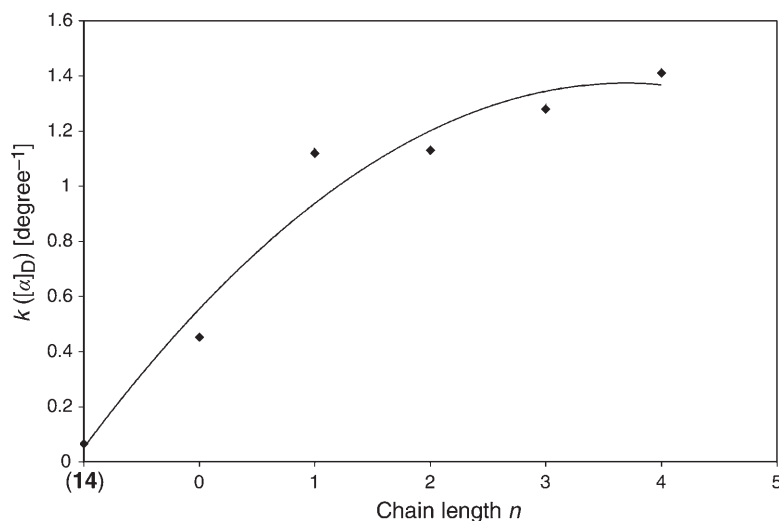


Fig. 3. Dependency of the temperature dependency k of the optical rotation $k ([\alpha]_D)^\circ$ with the chain length n

further increase for the dimer **17**. For the trimer **18**, tetramer **19**, and pentamer **20**, the value of the specific optical rotation remains approximately the same.

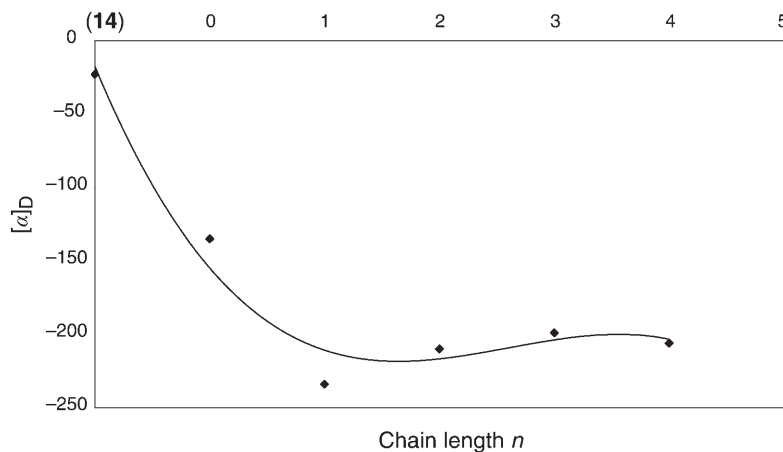


Fig. 4. Dependency of the optical rotation $[\alpha]_D$ with the chain length

By measuring the dependency k of the optical rotation with the temperature at 436 nm, the same tendency as described above for the measurement at 589 nm was observed, with approximately two times higher values (data not shown). All the measurements were reversible within a range of 20° to 50°. The strong temperature dependency of the optical rotation of the oligomers **16–20** and the high optical rotations of **16–20** in comparison to that of **14** are a clear evidence for the ordered structure of the oxymethylene units in the oligomers **16–20**.

4. *Molecular Modeling.* To get a first idea about the way the conformation of our helix would be initiated by (1*S*)-2,2-dimethyl-1-phenylpropan-1-ol (**14**), we performed modeling calculations. First we calculated the right-handed conformation for the oxymethylene units in dimer **17** ($n = 1$). As starting conformation, we chose the b-pl-H rule conformation around the C(1)–O(2) as for the O(6)–C(7) bond¹), respectively (corresponding to an *anti*-periplanar (*ap*) arrangement of the *tert*-butyl groups and C(3) and C(5), resp.) and the +*sc* conformation around the other bonds along the helix. After the minimization, we examined the torsion angles along the chain. We found a significant deviation of the *ap* conformation for the C(1)–O(2) bond of 23° as well as a deviation from the *sc* conformation of 8° and 17° for the remaining bonds in the helix chain. This calculation was repeated with the same starting conformation around the C(1)–O(2) bond (and around the O(6)–C(7) bond) but with –*sc* conformation around the other bonds along the helix. After the minimization, we found here smaller deviations in the *ap* conformation for the C(1)–O(2) bond of 12° as well as for the deviation from the –*sc* conformation of 5° and 10° for the remaining bonds in the helix chain. Therefore, we concluded that if the helix is induced by **14**, we should end up with a left-handed conformation for the poly(oxymethylene) helix. These calculations were compared with the results of the X-ray structure analysis of dimer **17** and tetramer **19**.

Next, we performed the same calculations with pentamer **20**. As in the case of dimer **17**, we obtained, after the minimization of the right-handed case of the idealized structure, considerable deviations of the torsion angles of the C(1)–O(2) bond (*ca.* 30°) and deviations for the other bond angles in the helix from the +*sc* conformation (0–18°). In the case of the left-handed helix, we got smaller aberrations for the torsion angles of the C(1)–O(2) bond (*ca.* 10°) as well as for the other bond angles in the helix from the –*sc* conformation (2–5°). Therefore, we concluded again that these results give a clue about the preferred conformation of the helix in pentamer **20**.

5. *X-Ray Structure Analysis of Dimer 17 and Tetramer 19.* From dimer **17** and tetramer **19**, we obtained suitable crystals by recrystallization from EtOH for an X-ray analysis²).

For dimer **17**, the absolute structure could not be determined reliably (see poorly defined *Flack* parameter). However, since the absolute configuration of **14** is (*S*), corresponding to a ‘*B*-descriptor’ in the stereoelectronic-effect-based classification [19], we find from the optical rotation the left-handed conformation for the oxymethylene helix, as it was predicted by the calculations for dimer **17** (see *Fig. 5*). As expected, the torsion angles C(5)–C(1)–O(1)–C(2) (*Fig. 5, Table 1*) and C(3)–O(3)–C(4)–C(15) are 150.1(2) and 156.9(2)°, respectively, with a deviation of 30° and 23°, respectively, from the b-pl-H rule.

The remaining torsion angles in the poly(oxymethylene) helix of **17** are in the expected range of –69° to –79° resulting in a deviation of 9–19° from the idealized conformation according to the anomeric effect as shown by the calculations. The

²) CCDC-658327 (**17**) and CCDC-658328 (**19**) contain the supplementary crystallographic data for this paper. These data can be obtained free of charge via http://www.ccdc.cam.ac.uk/data_request/cif (or from the *Cambridge Crystallographic Data Centre*, 12 Union Road, Cambridge CB2 1EZ, UK; fax: +44(1223)336033; e-mail: deposit@ccdc.cam.ac.uk).

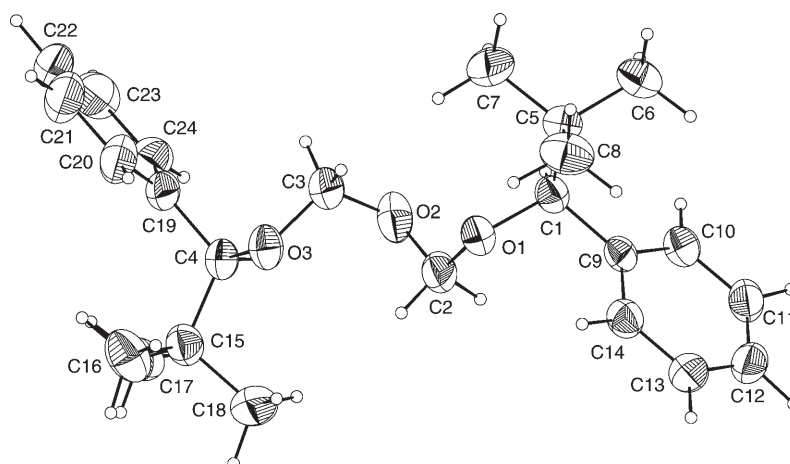


Fig. 5. Structure of **17** obtained by X-ray diffraction. Thermal ellipsoids at 50% level; H-atoms shown as small spheres of arbitrary radii; drawings performed with ATOMS [30].

Table 1. Selected Bond Lengths, Bond Angles, and Torsion Angles of **17**. See Fig. 5 for atom numbering.

Length [Å]		Angle [°]		Torsion angle [°]	
C(1)–O(1)	1.447(2)	C(1)–O(1)–C(2)	113.5(2)	C(5)–C(1)–O(1)–C(2)	150.1(2)
O(1)–C(2)	1.399(3)	O(1)–C(2)–O(2)	112.9(2)	C(1)–O(1)–C(2)–O(2)	–79.4(2)
C(2)–O(2)	1.406(3)	C(2)–O(2)–C(3)	112.0(2)	O(1)–C(2)–O(2)–C(3)	–69.4(2)
O(2)–C(3)	1.412(3)	O(2)–C(3)–O(3)	112.0(2)	C(2)–O(2)–C(3)–O(3)	–72.6(2)
C(3)–O(3)	1.404(3)	C(3)–O(3)–C(4)	113.2(2)	O(2)–C(3)–O(3)–C(4)	–76.4(2)
O(3)–C(4)	1.439(3)			C(3)–O(3)–C(4)–C(15)	156.9(2)

C–O–C bond angles are almost constant and within the range 113.5(2)–112.0(2)°. The O–C–NO bond angles are also almost constant with 112.9(2) and 112.0(2)°. No stereoelectronic effects are expected for the terminal C–O bonds. Those bonds show a length of 1.447(2) and 1.439(3) Å, and thus are significantly longer than the remaining C–O bonds which are in the range 1.399(3)–1.412(3) Å. This shortening of *ca.* 0.038 Å with respect to a standard C–O bond indicates a clear operating anomeric effect and indicates a C=O bond character of *ca.* 28%.

For tetramer **19**, we observed a similar picture as in the case of dimer **17** (Fig. 6, Table 2). Similarly, the refinement of the tetramer **19** did not allow a reliable determination of the absolute structure. But since the absolute configuration of **14** is known from the specific rotation as mentioned above, we can define a left-handed conformation for the poly(oxyethylene) helix of **19**, as predicted by the calculations and shown in Fig. 6. As for **17**, no steric effect is operating for the terminal C–O bonds. These bonds show a length of 1.436(4) and 1.402(5) Å, and are again significantly longer than the remaining C–O bonds, which are within the range 1.370(5)–1.416(5) Å. This shortening of *ca.* 0.027 Å with respect to a standard C–O bond indicates again the operating anomeric effect. The torsion angles C(7)–C(1)–O(1)–C(2) and C(5)–O(5)–C(6)–C(17) are 161.8(3) and 149.2(4)°, respectively, with a deviation

of 18° and 31° , respectively, according to the b-pl-H rule. The remaining torsion angles in the poly(oxyethylene) helix lie within the expected range (-65° to -90°), resulting in a deviation of up to 30° from the idealized conformation according to the anomeric effect, as shown by the calculations. The C–O–C bond angles are almost constant and in the range of 113 – 115° . The O–C–O bonds are also almost constant within 111° and 115° .

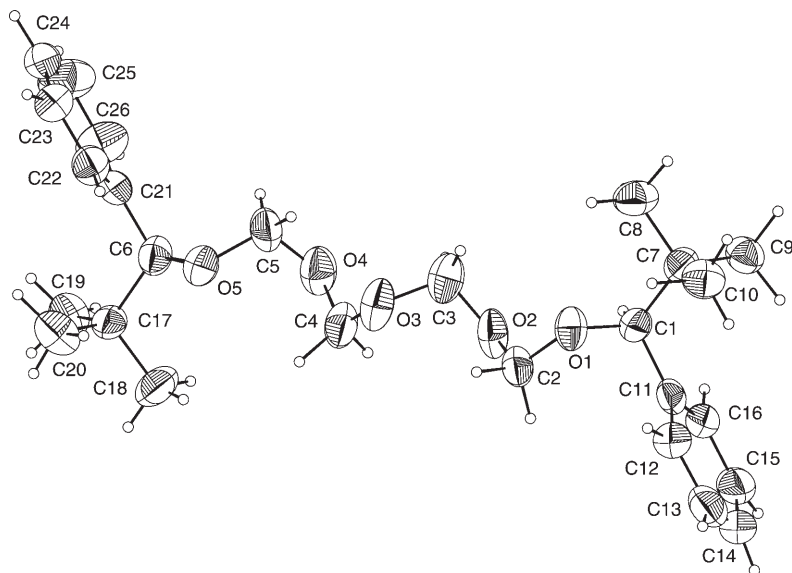


Fig. 6. Structure of **19** obtained by X-ray diffraction. Thermal ellipsoids at 50% level; H-atoms shown as small spheres of arbitrary radii; drawings performed with ATOMS [30]. Arbitrary atom numbering.

Table 2. Selected Bond Lengths, Bond Angles, and Torsion Angles of **19**. See Fig. 6 for atom numbering.

Length [Å]		Angle [°]		Torsion angle [°]	
C(1)–O(1)	1.436(4)	C(1)–O(1)–C(2)	113.1(3)	C(7)–C(1)–O(1)–C(2)	161.8(3)
O(1)–C(2)	1.411(4)	O(1)–C(2)–O(2)	113.7(4)	C(1)–O(1)–C(2)–O(2)	–67.1(5)
C(2)–O(2)	1.388(5)	C(2)–O(2)–C(3)	114.1(4)	O(1)–C(2)–O(2)–C(3)	–78.7(5)
O(2)–C(3)	1.392(6)	O(2)–C(3)–O(3)	111.1(4)	C(2)–O(2)–C(3)–O(3)	–80.1(5)
C(3)–O(3)	1.416(5)	C(3)–O(3)–C(4)	112.7(4)	O(2)–C(3)–O(3)–C(4)	–77.6(5)
O(3)–C(4)	1.409(6)	O(3)–C(4)–O(4)	114.7(4)	C(3)–O(3)–C(4)–O(4)	–74.1(6)
C(4)–O(4)	1.370(5)	C(4)–O(4)–C(5)	113.4(4)	O(3)–C(4)–O(4)–C(5)	–64.9(5)
O(4)–C(5)	1.406(6)	O(4)–C(5)–O(5)	112.1(4)	C(4)–O(4)–C(5)–O(5)	–71.2(5)
C(5)–O(5)	1.414(5)	C(5)–O(5)–C(6)	114.5(4)	O(4)–C(5)–O(5)–C(6)	–90.3(5)
O(5)–C(6)	1.402(5)			C(5)–O(5)–C(6)–C(17)	149.2(4)

Conclusions. – We synthesized a set of enantiomerically pure poly(oxyethylene) helices with predictable handedness, which are capped by moieties derived from (1*S*)-2,2-dimethyl-1-phenylpropan-1-ol (**14**), up to a pentamer **20**. By measuring the temperature-dependent optical rotation and temperature-dependent $^1\text{H-NMR}$ shifts,

we found a reversibility of an ordered structure that breaks down as soon as the temperature is increased, thus confirming the helical structure of the molecules in solution. In the X-ray structure analysis of dimer **17** and tetramer **19**, the helical arrangement of the oxymethylene units induced by the anomeric effect could also be found. Starting from **14** corresponding to a 'B'-descriptor according to the b-pl-H rule, we were able to establish the left-handedness of all the poly(oxymethylene) helices, which we could isolate and investigate. The option to directly correlate a B-type center of chirality to a left-handed helix may also be of importance in planning syntheses of enantiomerically pure oligo- and poly(acetals). Last but not least, it should be mentioned that in the case of an oxymethylene chain, helix chirality is introduced into an organic molecule by conformational order caused by stereoelectronic effects. Conditions for such an induction might easily be given by environmental circumstances, such as the presence of chiral inorganic molecules. The direct association of the handedness of a helix and the configuration of a chirality center bearing ligands, a situation frequently found in biomolecules, would then unambiguously define the direction of the propagation of this chirality.

Experimental Part

General. THF was distilled from Na/benzophenone, toluene from Na. Petroleum ether was of b.p. 50–75°. Reactions were run under Ar. Qual. TLC: precoated silica-gel plates (*Merck silica gel 60 F₂₅₄*): detection by spraying with 'mostain' (400 ml of 10% aq. H₂SO₄ soln., 20 g of (NH₄)₆Mo₇O₂·H₂O, 0.4 g of Ce(SO₄)₂) and heating. Flash chromatography (FC): silica gel *Merck 60* (0.04–0.063 mm). Optical rotations: 1-dm cell at 20° (unless otherwise given) and 589 nm. FT-IR: 1–2% KBr plates. ¹H- and ¹³C-NMR: at 200, 300, or 500 MHz and 50 or 125 MHz, resp. MS: Electron-spray ionization (ESI). All molecular-modeling calculations were performed with the *Pro™ Plus* program (version 6.2.2) of *ChemSW* (Fairfield, CA 94534).

(2R,3aR,4R,7S,7aR)-Hexahydro-2-hydroxy-8,8-dimethyl-N,N-bis(phenylmethyl)-4,7-methanobenzofuran-7(4H)-methanesulfonamide (**2**). At –78°, a soln. of *exo*-lactone **1** (4 g, 8.83 mmol) in toluene (60 ml) was treated dropwise with a soln. of 20% DIBAL in toluene (1.7 equiv., 15.0 mmol) in a way that the temp. did not exceed –40° and stirred for 2 h at –60°. The soln. was poured into ice (50 g) and 2N HCl (60 g), and the aq. phase was extracted with CH₂Cl₂ (2 ×). The combined org. phase was washed with sat. aq. NaHCO₃ soln. and H₂O, dried (Na₂SO₄), and concentrated: 3.6 g (90%) of **2**. Colorless crystals. *R_f* (petroleum ether/Et₂O 1:1) 0.39. M.p. 129–130°. IR: 3282*m* (br.), 2935*m*, 1453*m*, 1332*s*, 1143*s*, 1089*m*, 1042*m*, 1013*m*, 934*m*, 792*m*, 702*m*. ¹H-NMR (200 MHz, CDCl₃): 7.35–7.30 (*m*, 10 arom. H); 5.40 (*d*, *J* = 3.4, H–C(2)); 4.60 (*d*, *J* = 7.6, H–C(7a)); 4.40 (*d*, *J* = 15.1, PhCH₂N); 4.29 (*d*, *J* = 15.1, PhCH₂N); 3.26 (*d*, *J* = 13.6, 1 H, SO₂CH₂C(7)); 2.67 (br. *s*, OH); 2.67 (*d*, *J* = 13.5, 1 H, SO₂CH₂C(7)); 2.52–2.38 (*m*, H–C(3a)); 2.20–1.65 (*m*, H–C(7a)); 2.20–1.65 (*m*, 1 H–C(5), 1 H–C(6), CH₂(3), H–C(4)); 1.60–1.40 (*m*, 1 H–C(5)); 1.20–1.00 (*m*, 1 H–C(6)); 0.81, 0.71 (2*s*, Me₂C). ¹³C-NMR (50 MHz, CDCl₃): 136.0 (*s*, C(1) of Ph); 129.1 (*d*, C(2,6) of Ph); 128.8 (*d*, C(3,5) of Ph); 128.0 (*d*, C(4) of Ph); 99.8 (*d*, C(2)); 87.6 (*d*, C(7a)); 51.6 (*t*, SO₂CH₂–C(7)); 50.1 (*t*, PhCH₂N); 49.4 (*s*, C(8)); 48.5 (*s*, C(7)); 47.6 (*d*, C(4)); 46.1 (*t*, C(3)); 39.3 (*d*, C(3a)); 29.0 (*t*, C(5)); 28.6 (*t*, C(6)); 23.2, 20.4 (2*q*, Me₂C). ESI-MS (pos.-ion mode): 949 (20, [2*M* + K]⁺), 933 (100, [2*M* + Na]⁺), 494 (7, [*M* + K]⁺), 478 (15, [*M* + Na]⁺). Anal. calc. for C₂₆H₃₃NO₄S (455.61): C 68.54, H 7.30, N 3.07, S 7.04; found: C 68.44, H 7.53, N 3.16, S 6.84.

(2R,3aR,4R,7S,7aR)-Hexahydro-8,8-dimethyl-N,N-bis(phenylmethyl)-2-[(1*S*)-1-phenylpropoxy]-4,7-methanobenzofuran-7(4H)-methanesulfonamide (**3**). A soln. of (±)-**4** (4.31 ml, 31.5 mmol) and **2** (3.6 g, 7.9 mmol) in CH₂Cl₂ (25 ml) was treated with triphenylphosphonium bromide (343 mg, 1 mmol) and stirred at 23° for 20 h. The mixture was washed with sat. aq. NaHCO₃ soln. and brine, dried (Na₂SO₄), and concentrated. FC (petroleum ether/BuOMe 30:1–6:1) gave **3** (2.11 g, 49%) and **3'**

diastereoisomer of **3** (1.35 g, 31.3%). Data of **3**: Colorless oil. R_f (petroleum ether/Et₂O 3:1) 0.68. $[\alpha]_D^{25} = -84.5$ ($c = 0.99$, acetone). IR: 2903s, 1495m, 1456m, 1336s, 1148s, 1009m, 790m, 701s. ¹H-NMR (200 MHz, CDCl₃): 7.60–7.20 (*m*, 15 arom. H); 4.97 (*d*, $J = 4.7$, H–C(2)); 4.58 (*d*, $J = 7.7$, H–C(7a)); 4.57–4.54 (*m*, H–C(1')); 4.58 (*d*, $J = 15.1$, PhCH₂N); 4.32 (*d*, $J = 15.1$, PhCH₂N); 3.26 (*d*, $J = 13.5$, 1 H, SO₂CH₂–C(7)); 2.62 (*d*, $J = 13.5$, 1 H, SO₂CH₂–C(7)); 2.55–2.28 (*m*, H–C(3a)); 2.20–1.65 (*m*, H–C(7a)); 2.20–1.50 (*m*, CH₂(5), CH₂(6), CH₂(3), H–C(4), CH₂(2')); 0.92 (*t*, $J = 7.7$, Me(3')); 0.77, 0.73 (2s, Me₂C). ¹³C-NMR (50 MHz, CDCl₃): 142.0 (*s*, C(1) of Ph); 136.1 (*s*, C(1) of Bn); 129.2 (*d*, C(2,6) of Bn); 128.8 (*d*, C(3,5) of Bn); 128.3 (*d*, C(2,6) of Ph); 128.1 (*d*, C(3,5) of Ph); 127.3 (*d*, C(4) of Ph); 127.2 (*d*, C(4) of Bn); 101.5 (*d*, C(2)); 87.0 (*d*, C(7a)); 78.1 (*d*, C(1')); 51.8 (*t*, SO₂CH₂–C(7)); 50.0 (*t*, PhCH₂N); 49.4 (*s*, C(8)); 48.5 (*s*, C(7)); 47.7 (*d*, C(4)); 46.4 (*t*, C(3)); 38.8 (*d*, C(3a)); 31.5 (*t*, C(2')); 29.1 (*t*, C(5)); 28.4 (*t*, C(6)); 23.2, 20.4 (2*q*, Me₂C); 10.9 (*q*, C(3')).

(1*S*)-1-Phenylpropan-1-ol (**4**). A soln. of **3** (4.8 g, 8.8 mmol) in CH₂Cl₂ (6 ml) and ⁱPrOH (18 ml) was treated with TsOH·H₂O (1 g, 5.3 mmol) and stirred at 23° for 100 h. The mixture was diluted with AcOEt (50 ml), washed with sat. aq. NaHCO₃ soln. and brine, dried (Na₂SO₄), and concentrated, and the residue purified by bulb-to-bulb distillation: **4** (558 mg, 47%).

Data of **4**: Colorless oil. R_f (petroleum ether/Et₂O 15:1) 0.20. $[\alpha]_D^{25} = -30.1$ ($c = 0.85$, acetone). IR: 3370m (br.), 2964m, 2930m, 2860m, 1492m, 1453s, 1096m, 1013m, 775m, 763m, 700s. ¹H-NMR (200 MHz, CDCl₃): 7.45–7.25 (*m*, 5 arom. H); 4.59 (*t*, $J = 6.7$, H–C(1)); 1.88 (*quint.*, $J = 8.8$, 1 H–C(2)); 1.74 (*quint.*, $J = 9.0$, 1 H–C(2)); 0.93 (*t*, $J = 7.3$, Me(3)). ¹³C-NMR (50 MHz, CDCl₃): 144.7 (*s*, C(1) of Ph); 128.5 (*d*, C(2,6) of Ph); 127.6 (*d*, C(3,5) of Ph); 126.1 (*d*, C(4) of Ph); 76.1 (*d*, C(1)); 32.0 (*t*, C(2)); 10.3 (*q*, C(3)). ESI-MS (pos.-ion mode): 159 (20, [M + Na]⁺).

Data of (2*R*,3*aR*,4*R*,7*S*,7*aR*)-Hexahydro-8,8-dimethyl-2-(1-methylethoxy)-N,N-bis(phenylmethyl)-4,7-methanobenzofuran-7(4*H*)-methanesulfonamide (**5**): Colorless oil. R_f (petroleum ether/Et₂O 15:1) 0.36. ¹H-NMR (200 MHz, CDCl₃): 7.50–7.20 (*m*, 10 arom. H); 5.25 (*d*, $J = 3.5$, H–C(2)); 4.48 (*d*, $J = 7.6$, H–C(7a)); 4.50 (*d*, $J = 15.2$, PhCH₂N); 4.37 (*d*, $J = 13.5$, PhCH₂N); 3.97 (*sept.*, $J = 6.2$, Me₂CH–C(2)); 3.30 (*d*, $J = 13.5$, 1 H, SO₂CH₂–C(7)); 2.63 (*d*, $J = 13.5$, 1 H, SO₂CH₂–C(7)); 2.50–2.30 (*m*, H–C(3a)); 2.20–1.65 (*m*, H–C(7a)); 2.15–1.60 (*m*, 1 H–C(5), 1 H–C(6), CH₂(3), H–C(4)); 1.20 (*d*, $J = 7.7$, 3 H, Me₂CH–C(2)); 1.15–1.10 (*m*, 1 H–C(5)); 1.10 (*d*, $J = 6.1$, 3 H, Me₂CH–C(2)); 1.00–0.90 (*m*, 1 H–C(6)); 0.87, 0.74 (2s, Me₂C).

trans-5-Methyl-4-phenyl-1,3-dioxolane (**6**). A suspension of paraformaldehyde (12.0 g, 0.4 mol) and (±)-**4** (5.4 ml, 0.04 mol) in benzene (60 ml) was treated dropwise at 23° with H₂SO₄ (0.5 ml), stirred under reflux for 2 h, cooled to 23°, treated with solid NaHCO₃ (2 g), and stirred for 30 min. The mixture was filtered, the solid washed with ^tBuOMe, and the filtrate concentrated. FC (petroleum ether/^tBuOMe 60:1 → 6:1) gave **6** (5.74 g, 81%). Colorless oil. R_f (petroleum ether/Et₂O 15:1) 0.17. IR: 2959m, 2842m, 1494w, 1455m, 1402m, 1380m, 1175s, 1107m, 1072s, 1029s, 956m, 756m, 700s. ¹H-NMR (500 MHz, CDCl₃): 7.40–7.25 (*m*, 5 arom. H); 5.20 (*d*, $J_{gem} = 6.2$, 1 H–C(2)); 4.82 (*d*, $J_{gem} = 6.3$, 1 H–C(2)); 4.12 (*d*, $J = 10$, H–C(4)); 4.11 (*d*, $J = 11.1$, H_a–C(6)); 3.40 (*t*, $J_{gem} \approx {}^3J(6b,5) = 11.1$, H_b–C(6)); 2.18–2.05 (*m*, H–C(5)); 0.58 (*d*, $J = 8.8$, Me–C(5)). ¹³C-NMR (125 MHz, CDCl₃): 139.4 (*s*, C(1) of Ph); 128.3 (*d*, C(2,6) of Ph); 128.1 (*d*, C(4) of Ph); 127.2 (*d*, C(3,5) of Ph); 94.0 (*t*, C(2)); 86.1 (*d*, C(4)); 72.9 (*t*, C(6)); 36.3 (*d*, C(5)); 12.4 (*q*, Me).

1-(4-Nitrophenyl)ethanol (**8**). At 0°, a soln. of 4-nitroacetophenone (5 g, 30 mmol) in EtOH (30 ml) was treated dropwise with a soln. of NaBH₄ (0.34 g, 9.1 mmol) in EtOH (8 ml) and stirred for 1 h. The mixture was then treated with sat. aq. NH₄Cl soln. (15 ml), diluted with AcOEt (80 ml), washed with sat. aq. NH₄Cl soln. and brine, dried (Na₂SO₄), and concentrated: **8** (4.9 g, 98%). R_f (petroleum ether/Et₂O 1:1) 0.28. IR (KBr): 3399m (br.), 2975w, 1605m, 1519s, 1347s, 1107m, 1090m, 1013w, 856m, 700m. ¹H-NMR (200 MHz, CDCl₃): 8.16 (*d*, $J = 6.2$, H–C(3',5')); 7.52 (*d*, $J = 8.6$, H–C(2',6')); 5.01 (*q*, $J = 6.6$, H–C(1)); 2.20 (*s*, OH); 1.50 (*d*, $J = 6.6$, Me(2)). ¹³C-NMR (125 MHz, CDCl₃): 153.2 (*s*, C(4) of Ar); 146.0 (*s*, C(1) of Ar); 126.2 (*d*, C(2,6) of Ar); 123.8 (*d*, C(3,5) of Ar); 69.6 (*d*, C(1)); 25.6 (*q*, Me).

2,6-Bis(4-nitrophenyl)-3,5-dioxheptane (=1,1'-[Methylenebis(oxyethylidene)]bis[4-nitrobenzene]; **9**). A suspension of paraformaldehyde (3.6 g, 120 mmol) and (±)-**8** (2 g, 12 mmol) in benzene (20 ml) was treated dropwise at 23° with H₂SO₄ (0.13 ml), stirred under reflux for 2 h, cooled to 23°, treated with solid NaHCO₃ (0.5 g), and stirred for 30 min. The mixture was filtered, the solid washed with ^tBuOMe, and the filtrate evaporated. FC (petroleum ether/^tBuOMe 10:1 → 1:1) gave **9** (1.70 g, 83%). Yellow

crystals. R_f (petroleum ether/Et₂O 1:1) 0.28. M.p. 123–126°. IR (KBr): 3109w, 2979w, 1607m, 1520s, 1348s, 1105m, 1094m, 1024s, 1008m. ¹H-NMR (200 MHz, CDCl₃): 8.14 (*d*, $J = 8.6$, H–C(3',5')); 7.43 (*d*, $J = 8.6$, H–C(2',6')); 4.91 (*q*, $J = 6.6$, H–C(2,6)); 4.55 (*s*, OCH₂O); 1.49 (*d*, $J = 6.6$, 2 Me). ¹³C-NMR (50 MHz, CDCl₃): 150.8 (*s*, C(4) of Ar); 147.5 (*s*, C(1) of Ar); 127.2 (*d*, C(2,6) of Ar); 123.9 (*d*, C(3,5) of Ar); 91.2 (*t*, OCH₂O); 73.6 (*d*, C(1,5)); 25.6 (*q*, Me). ESI-MS (pos.-ion mode): 369.1 (100, [M + Na]⁺). Anal. calc. for C₁₇H₁₈N₂O₄ (346.12): C 58.96, H 5.24, N 8.09; found: C 59.21, H 5.31, N 7.98.

(4*a*R,4*b*S,5*R*,8*S*,8*a*R,9*a*S)-Hexahydro-10,10-dimethyl-N,N-bis(phenylmethyl)-5,8-methano-4*H*-1,3-dioxino[4,5-*b*]benzofuran-8(5*H*)-methanesulfonamide (**10**). A suspension of paraformaldehyde (1.3 g, 40 mmol) and **2** (2 g, 4.4 mmol) in benzene (15 ml) was treated dropwise at 23° with H₂SO₄ (0.05 ml), stirred under reflux for 1 h, cooled to 23°, treated with solid NaHCO₃ (0.2 g), and stirred for 1 h. The mixture was filtered, the solid washed with ^tBuOMe, and the filtrate evaporated. FC (petroleum ether/^tBuOMe 3:1 → 1:2) gave **10** (0.93 g, 37%). Yellow foam. $[\alpha]_D^{25} = 4$ ($c = 1.0$, acetone). R_f (petroleum ether/Et₂O 1:1) 0.16. IR: 2935m, 1494w, 1455w, 1334s, 1147s, 1111s, 1038m, 1014m, 918m, 892m, 791m, 704m. ¹H-NMR (500 MHz, CDCl₃): 7.36–7.25 (*m*, 10 arom. H); 5.25 (*d*, $J = 3.5$, H–C(9*a*)); 4.96 (*d*, $J = 7.0$, 1 H, H–C(2)); 4.72 (*d*, $J = 7.6$, H–C(8*a*)); 4.63 (*d*, $J = 6.6$, 1 H, H–C(2)); 4.42 (*d*, $J = 15.2$, PhCH₂N); 4.32 (*d*, $J = 15.2$, PhCH₂N); 4.07 (*d*, $J = 12.3$, 1 H, H–C(4)); 3.90 (*dd*, $J = 12.0, 3.5$, 1 H, H–C(4)); 3.26 (*d*, $J = 13.6$, 1 H, SO₂CH₂–C(8)); 2.65 (*d*, $J = 13.6$, 1 H, SO₂CH₂–C(8)); 2.40 (*t*, $J = 7.9$, H–C(4*b*)); 2.23 (*dt*, $J = 3.2, 7.9$, H–C(4*a*)); 1.92 (*td*, $J = 3.8, 11.7$, 1 H, H–C(7)); 1.81 (*tt*, $J = 3.8, 12.0$, 1 H, H–C(6)); 1.75 (*d*, $J = 4.1$, H–C(5)); 1.52 (*td*, $J = 4.5, 13.2$, 1 H, H–C(7)); 1.16 (*dt*, $J = 3.8, 12.3$, 1 H, H–C(6)); 0.91, 0.79 (2*s*, Me₂C). ¹³C-NMR (125 MHz, CDCl₃): 135.9 (*s*, C(1) of Ph); 129.0 (*d*, C(2,6) of Ph); 128.5 (*d*, C(3,5) of Ph); 127.8 (*d*, C(4) of Ph); 99.8 (*d*, C(9*a*)); 90.3 (*t*, OCH₂O); 89.2 (*d*, C(8*a*)); 66.9 (*t*, C(4)); 51.0 (*t*, SO₂CH₂–C(8)); 49.9 (*t*, PhCH₂N); 49.5 (*s*, C(10)); 49.2 (*d*, C(4*b*)); 48.3 (*s*, C(8)); 46.6 (*d*, C(5)); 45.0 (*d*, C(4*a*)); 28.9 (*t*, C(6)); 28.2 (*t*, C(7)); 23.1, 20.8 (2*q*, Me₂C). ESI-MS (pos.-ion mode): 536 (70, [M + K]⁺), 520 (100, [M + Na]⁺). Anal. calc. for C₂₈H₃₅NO₅S (497.22): C 67.38, H 7.09, N 2.81; found: 67.65, H 7.16, N 2.67.

(2*R*,3*a*R,4*R*,7*R*,7*a*R)-Octahydro-7,8,8-trimethyl-4,7-methanobenzofuran-2-ol (**12**) and (2*S*,3*a*R,4*R*,7*R*,7*a*R)-Octahydro-7,8,8-trimethyl-4,7-methanobenzofuran-2-ol (C(2)-anomer of **12**). At –78°, a soln. of *exo*-lactone **11** (5.83 g, 30 mmol) in toluene (100 ml) was treated dropwise with a soln. of 20% DIBAL in toluene (35 ml, 1.7 equiv., 51 mmol) such that the temp. did not exceed –40° and stirred for 3 h at –60°. The soln. was poured into ice (50 g) and 2*N* HCl (100 ml) and the aq. phase extracted with AcOEt (2 ×). The combined org. phase was washed with sat. aq. NaHCO₃ soln. and brine, dried (Na₂SO₄), and concentrated: 5.3 g (91%) of **12**. Colorless crystals. R_f (petroleum ether/Et₂O 1:1) 0.47. M.p. 68–70°. IR: 3404m (br.), 2951s, 1482m, 1450m, 1089s, 1020s, 946s. ¹H-NMR (200 MHz, CDCl₃): mixture of **12** and anomer: 5.56 (*t*, $J = 2.0$, H–C(2)); 5.40 (*d*, $J = 3.9$, H–C(2) of anomer); 4.08 (*d*, $J = 7.6$, H–C(7*a*)); 3.80 (*d*, $J = 3.8$, H–C(7*a*) of anomer); 2.39–1.30 (*m*, H–C(3*a*), H–C(3), H–C(4), CH₂(5), CH₂(6)); 0.96, 0.95 (*s*, Me₂C); 0.82, 0.81 (2*s*, Me–C(7)). ¹³C-NMR (50 MHz, CDCl₃): 101.0 (*d*, C(2)); 100.2 (*d*, C(2) of anomer); 91.9 (*d*, C(7*a*) of anomer); 91.6 (*d*, C(7*a*)); 48.5 (*s*, C(8)); 48.0 (*d*, C(4)); 47.4 (*t*, C(3)); 46.4 (*s*, C(7)); 46.1 (*s*, C(7) of anomer); 39.6 (*d*, C(3*a*)); 38.8 (*d*, C(3*a*) of anomer); 32.8 (*t*, C(5)); 29.3 (*t*, C(6)); 23.3, 20.94 (2*q*, Me₂C), 12.1, 11.9 (2*q*, Me–C(7)).

(2*S*,3*a*R,4*R*,7*R*,7*a*R)-2-[(1*S*)-2,2-Dimethyl-1-phenylpropoxy]octahydro-7,8,8-trimethyl-4,7-methanobenzofuran (**13**). A soln. of (±)-**14** (8.0 g, 48.7 mmol) and lactol **12** (2.39 g, 12.2 mmol) in CH₂Cl₂ (10 ml) was treated with triphenylphosphonium bromide (837 mg, 2.4 mmol) and stirred at 23° for 72 h. The mixture was diluted with AcOEt (50 ml), washed with sat. aq. NaHCO₃ soln. and brine, dried (Na₂SO₄), and concentrated. FC (petroleum ether/^tBuOMe 200:1 → 20:1) gave **13** (1.58 g, 38%) and **13**/diastereoisomer of **13** (2.0, 49%). **13**: Colorless oil. R_f (petroleum ether/Et₂O 70:1) 0.21. $[\alpha]_D^{25} = -137$ ($c = 0.33$, acetone). IR (KBr): 2955s, 1480m, 1450m, 1362s, 1188m, 1069m, 1022s, 956m, 739m, 702m. ¹H-NMR (200 MHz, CDCl₃): 7.30–7.20 (*m*, 5 arom. H); 4.84 (*d*, $J = 4.9$, H–C(2)); 4.30 (*s*, H–C(1')); 3.94 (*d*, $J = 7.4$, H–C(7*a*)); 2.36–1.35 (*m*, H–C(3*a*), H_a–C(5), H_a–C(6), CH₂(3), H–C(4)); 1.10–0.85 (*m*, H_b–C(5), H_b–C(6)); 1.00 (*s*, 3 H, Me₂C), 0.82 (*s*, Me₂C); 0.81 (*s*, Me–C(7)); 0.77 (*s*, 3 H, Me₂C). ¹³C-NMR (50 MHz, CDCl₃): 140.1 (*s*, C(1) of Ph); 129.0 (*d*, C(2,6) of Ph); 127.4 (*d*, C(3,5) of Ph); 127.0 (*d*, C(4) of Ph); 102.0 (*d*, C(2)); 91.3 (*d*, C(7*a*)); 83.7 (*d*, C(1')); 48.6 (*s*, C(8)); 47.7 (*d*, C(4)); 47.1 (*t*, C(3)); 46.3 (*s*, C(7)); 38.6 (*d*, C(3*a*)); 35.2 (*s*, C(2')); 32.3 (*t*, C(6)); 29.1 (*t*, C(5)); 25.0 (*t*, C(3')); 23.1, 20.6 (2*q*, Me₂C); 11.9 (*q*, Me–C(7)). Anal. calc. for C₂₃H₃₄O₂ (342.51): C 80.65, H 10.01; found: 80.51, H 9.74.

(*1S*)-2,2-Dimethyl-1-phenylpropan-1-ol (**14**). A soln. **13** (1.56 g, 4.6 mmol) in CH₂Cl₂ (4 ml) and MeOH (4 ml) was treated with TsOH·H₂O (35 mg, 0.2 mmol) and stirred at 23° for 20 h. The mixture was diluted with AcOEt (50 ml), washed with sat. aq. NaHCO₃ soln. and brine, dried (Na₂SO₄), and concentrated. FC (petroleum ether/BuOMe 75 : 1 → 2 : 1) gave **14** (500 mg, 67%).

Data of 14: Colorless crystals. M.p. 55–56°. *R*_f (petroleum ether/Et₂O 15 : 1) 0.23. [α]_D²⁵ = –22.7 (*c* = 0.75, acetone). IR (KBr): 3420s (br.), 2952m, 1479m, 1452m, 1304w, 1236w, 1179w, 1044m, 1003s, 737s, 701s. ¹H-NMR (200 MHz, CDCl₃): 7.35–7.15 (*m*, 5 arom. H); 4.35 (*s*, H–C(1)); 1.90 (*s*, OH); 0.95 (*s*, Me₃C). ¹³C-NMR (50 MHz, CDCl₃): 142.3 (*s*, C(1) of Ph); 127.7 (*d*, C(2,6) of Ph); 127.6 (*d*, C(3,5) of Ph); 127.41 (*d*, C(4) of Ph); 82.5 (*d*, C(1)); 35.7 (*t*, C(2)); 26.0 (*q*, C(3)). ESI-MS (pos.-ion mode): 187 (15, [M + Na]⁺). Anal. calc. for C₁₁H₁₆O (164.24): C 80.44, H 9.82; found: 80.31, H 9.82.

Data of (2R,3aR,4R,7R,7aR)-Octahydro-2-methoxy-7,8,8-trimethyl-4,7-methanobenzofuran (15): Colorless oil. *R*_f (petroleum ether/Et₂O 1 : 1) 0.50. [α]_D²⁵ = –125.3 (*c* = 0.70, acetone). IR (KBr): 2947s, 2825w, 1478m, 1447m, 1391m, 1347m, 1212m, 1108s, 1073m, 1034s, 955s, 886m. ¹H-NMR (200 MHz, CDCl₃): 4.99 (*t*, *J* = 2.4, H–C(2)); 3.90 (*d*, *J* = 7.4, H–C(7a)); 3.29 (*s*, MeO); 2.28 (*q*, *J* = 8.5, H–C(3a)); 2.05 (*d*, *J* = 2.6, H_a–C(3)); 2.02–2.00 (*m*, H_b–C(3)); 1.80–1.60 (*m*, H_a–C(6), H–C(4)); 1.42 (*m*, H_a–C(5)); 1.03–0.88 (*m*, H_b–C(5), H_b–C(6)); 0.98, 0.96 (2s, Me₂C); 0.79 (*s*, Me–C(7)).

(*1S,5S*)-1,5-Di(tert-butyl)-1,5-diphenyl-2,4-dioxapentane (= 1,1'-{Methylenebis[oxyl(*1S*)-2,2-dimethylpropylidene]}bis[benzene]; **16**), (*1S,7S*)-1,7-Di(tert-butyl)-1,7-diphenyl-2,4,6-trioxaheptane (= 1,1'-{Oxybis[methyleneoxyl(*1S*)-2,2-dimethylpropylidene]}bis[benzene]; **17**), (*1S,9S*)-1,9-Di(tert-butyl)-1,9-diphenyl-2,4,6,8-tetraoxanonane (= (*3S,11S*)-2,2,12,12-Tetramethyl-3,11-diphenyl-4,6,8,10-tetraoxatridecane; **18**), (*1S,11S*)-1,11-Di(tert-butyl)-1,11-diphenyl-2,4,6,8,10-pentaoxaundecane (= (*3S,13S*)-2,2,14,14-Tetramethyl-3,13-diphenyl-4,6,8,10,12-pentaoxapentadecane; **19**), (*1S,13S*)-1,13-Di(tert-butyl)-1,13-diphenyl-2,4,6,8,10,12-hexaoxatridecane (= (*3S,15S*)-2,2,16,16-Tetramethyl-3,15-diphenyl-4,6,8,10,12,14-hexaoxaheptadecane; **20**). A suspension of paraformaldehyde (0.89 g, 30 mmol) and **14** (489 mg, 3.0 mmol) in benzene (4 ml) was treated dropwise at 23° with H₂SO₄ (4 drops), stirred under reflux for 5 min, treated immediately with solid NaHCO₃ (0.4 g), and stirred for 30 min. The mixture was filtered, the solid washed with t-BuOMe, and the filtrate evaporated. FC (petroleum ether/BuOMe 200 : 1 → 0 : 2) and prep. TLC (petroleum ether/BuOMe 15 : 1 for **16**, **17**, and **18** and petroleum ether/BuOMe 6 : 1 for **20**) gave **16** (61 mg, 12%), **17** (98 mg, 18%), **18** (46 mg, 7.7%), **19** (49 mg, 7.6%), and **20** (9 mg, 1.3%).

Data of 16: Colorless oil. *R*_f (petroleum ether/Et₂O 15 : 1) 0.77. [α]_D²⁵ = –134 (*c* = 0.25, acetone). IR: 2956w, 1478w, 1451w, 1391w, 1360w, 1194w, 1155w, 1040s, 1020s, 740m, 703m. ¹H-NMR (200 MHz, CDCl₃): 7.26–7.15 (*m*, 10 arom. H); 4.41 (*s*, OCH₂O); 4.36 (*s*, H–C(1,5)); 0.92 (*s*, Me₃C–C(1,5)). ¹³C-NMR (50 MHz, CDCl₃): 139.2 (*s*, C(1) of Ph); 129.1 (*d*, C(2,6) of Ph); 127.5 (*d*, C(3,5) of Ph); 127.3 (*s*, C(4) of Ph); 89.7 (*t*, OCH₂O); 85.1 (*d*, C(1,5)); 26.7 (*q*, Me₃C); signal of Me₃C not found. ESI-MS (pos.): 363 (15, [M + Na]⁺).

Data of 17: Colorless crystals. *R*_f (petroleum ether/Et₂O 15 : 1) 0.57. [α]_D²⁵ = –229 (*c* = 0.52, acetone). M.p. 123–127°. IR: 2970s, 2897m, 1480m, 1451w, 1393m, 1365m, 1200m, 1138m, 1095s, 969s, 938m, 775m, 705s. ¹H-NMR (200 MHz, CDCl₃): 7.32–7.17 (*m*, 10 arom. H); 4.96 (*d*, *J* = 7.1, 2 H_a, OCH₂O); 4.36 (*d*, *J* = 7.1, 2 H_b, OCH₂O); 4.27 (*s*, H–C(1,7)); 0.85 (*s*, Me₃C–C(1,7)). ¹³C-NMR (50 MHz, CDCl₃): 139.2 (*s*, C(1) of Ph); 129.0 (*d*, C(2,6) of Ph); 127.6 (*d*, C(3,5) of Ph); 127.4 (*s*, C(4) of Ph); 88.3 (*t*, OCH₂O); 85.6 (*d*, C(1,7)); 35.0 (*s*, Me₃C); 26.7 (*q*, Me). ESI-MS (pos.): 393 (100, [M + Na]⁺).

Data of 18: Colorless crystals. *R*_f (petroleum ether/Et₂O 15 : 1) 0.30. M.p. 68–72°. [α]_D²⁵ = –208 (*c* = 0.21, acetone). IR: 2956m, 1478m, 1451m, 1391m, 1360m, 1190w, 1140s, 1040s, 1020s, 740m, 703m. ¹H-NMR (500 MHz, CDCl₃): 7.31–7.20 (*m*, 10 arom. H); 4.88 (*s*, OCH₂(5)O); 4.78 (*d*, *J* = 7.0, 2 H_a, OCH₂(3,7)O); 4.37 (*d*, *J* = 6.9, 2 H_b, OCH₂(3,7)O); 4.29 (*s*, H–C(1,9)); 0.89 (*s*, Me₃C–C(1,9)). ¹³C-NMR (125 MHz, CDCl₃): 139.0 (*s*, C(1) of Ph); 128.7 (*d*, C(2,6) of Ph); 127.5 (*d*, C(3,5) of Ph); 127.3 (*s*, C(4) of Ph); 89.0 (*t*, OCH₂(3,7)O); 87.4 (*t*, OCH₂(5)O); 85.7 (*d*, C(1,9)); 35.3 (*s*, Me₃C); 26.7 (*q*, Me₃C). ESI-MS (pos.): 423 (100, [M + Na]⁺).

Data of 19: Colorless crystals. *R*_f (petroleum ether/Et₂O 15 : 1) 0.20. M.p. 61–66°. [α]_D²⁵ = –193 (*c* = 0.20, acetone). IR: 2956m, 2904w, 1482m, 1452m, 1366m, 1119s, 1067m, 954s, 744m, 704m. ¹H-NMR (500 MHz, CDCl₃): 7.28–7.11 (*m*, 10 arom. H); 4.76 (*d*, *J* = 7.0, 2 H_a, OCH₂(5,7)O); 4.73 (*d*, *J* = 7.3, 2 H_a, OCH₂(3,9)O); 4.71 (*d*, *J* = 6.9, 2 H_b, OCH₂(5,7)O); 4.37 (*d*, *J* = 7.0, 2 H_b, OCH₂(3,9)O); 4.21 (*s*,

H–C(1,11)); 0.81 (*s*, Me₃C–C(1,11)). ¹³C-NMR (125 MHz, CDCl₃)¹: 139.0 (*s*, C(1) of Ph); 128.6 (*d*, C(2,6) of Ph); 127.4 (*d*, C(3,5) of Ph); 127.3 (*s*, C(4) of Ph); 89.5 (*t*, OCH₂(3,9)O); 88.1 (*t*, OCH₂(5,7)O); 86.1 (*d*, C(1,11)); 35.3 (*s*, Me₃C); 26.2 (*q*, Me). ESI-MS (pos.): 453 (100, [M + Na]⁺).

Data of 20: Colorless crystals. *R*_f (petroleum ether/Et₂O 15 : 1) 0.18. M.p. 86–91°. [*α*]_D²⁵ = –199 (*c* = 0.21, acetone). ¹H-NMR (500 MHz, CDCl₃)¹: 7.33–7.20 (*m*, 10 arom. H); 4.86 (*d*, *J* = 6.7, 2 H_a, OCH₂(5,9)O); 4.80 (*d*, *J* = 6.7, 2 H_b, OC(5,9)O); 4.79 (*d*, *J* = 6.3, 2 H_a, OCH₂(3,11)O); 4.78 (*s*, OCH₂(7)O); 4.46 (*d*, *J* = 7.0, 2 H_b, OCH₂(3,11)O); 4.28 (*s*, H–C(1,13)); 0.89 (*s*, Me). ¹³C-NMR (125 MHz, CDCl₃)¹: 139.0 (*s*, C(1) of Ph); 128.6 (*d*, C(2,6) of Ph); 127.5 (*d*, C(3,5) of Ph); 127.3 (*s*, C(4) of Ph); 89.7 (*t*, OCH₂(3,11)O); 88.7 (*t*, OCH₂(7)O); 88.3 (*t*, OCH₂(5,9)O); 86.2 (*d*, C(1,13)); 35.3 (*s*, Me₃C); 26.2 (*q*, Me₃C). ESI-MS (pos.): 483 (100, [M + Na]⁺).

Crystal Structure Determinations. Single-crystal X-ray diffraction data for **17** and **19** were measured at 200 K on a *Nonius-Kappa-CCD* diffractometer (graphite monochromatized MoK_α radiation) equipped with a 0.3 mm monochromatized collimator. The extraction and correction of the intensity data, including a pseudoabsorption correction by frame scaling and the refinement of lattice parameters, were performed with the program package DENZO-SMN [31]. For structure solutions by direct methods and the structure refinements, the programs SHELXS-97 [32] and SHELXL-97 [33] were used.

The structures were refined by full-matrix least-squares procedures on *F*². All non-H-atoms were refined with anisotropic displacement parameters. The H-atoms were localized from difference *Fourier* maps. Finally, idealized groups were used to describe the positions of the H-atoms with $U_{\text{H-atom}} = 1.2 \cdot U_{\text{equiv}}$ of the parent atom. Crystal parameters, details of data collection, and structure refinement are summarized in Table 3. In the case of **19**, a twin refinement was applied. Analysis of the final structure model gave no hints for a higher symmetry.

Table 3. Crystallographic Data for **17** and **19**

	17	19
Empirical formula	C ₂₄ H ₃₄ O ₃	C ₂₆ H ₃₈ O ₅
<i>M</i> _r	370.52	430.58
Crystal system	orthorhombic	monoclinic
Space group	<i>P</i> 2 ₁ 2 ₁ 2 ₁	<i>P</i> 2 ₁
<i>Z</i>	4	2
Unit cell parameters		
<i>a</i> [Å]	7.531(2)	6.007 (1)
<i>b</i> [Å]	10.945(2)	9.482 (2)
<i>c</i> [Å]	27.297(6)	22.145 (4)
<i>α</i> [°]	90	90
<i>β</i> [°]	90	90.02(3)
<i>γ</i> [°]	90	90
<i>V</i> [Å ³]	2250.1(8)	1261.4(4)
<i>ρ</i> [g/cm ³] (calc.)	1.094	1.134
<i>μ</i> [mm ^{−1}]	0.07	0.08
<i>F</i> (000)	808.0	468
2 θ _{max} [°]	50	52
Lim. indices	− 8 ≤ <i>h</i> ≤ 8, 12 ≤ <i>k</i> ≤ 13, − 32 ≤ <i>l</i> ≤ 32	− 7 ≤ <i>h</i> ≤ 7, − 11 ≤ <i>k</i> ≤ 11, − 27 ≤ <i>l</i> ≤ 27
Indep. refl.	3946	4866
Obs. refl. (<i>I</i> _o ≥ 2σ(<i>I</i>))	2636	2822
No. ref. param.	245	282
<i>wR</i> ₂ (all data)	0.098	0.113
<i>R</i> ₁ (<i>I</i> _o ≥ 2σ(<i>I</i>))	0.046	0.058
Goodness of fit (on <i>F</i> ²)	1.046	1.013
Δ <i>ρ</i> _{min} , Δ <i>ρ</i> _{max} [e/Å ³]	− 0.12, 0.13	− 0.12, 0.22

REFERENCES

- [1] H. Staudinger, M. Luthy, *Helv. Chim. Acta* **1925**, 8, 41.
[2] H. Staudinger, *Helv. Chim. Acta* **1925**, 8, 67.
[3] H. Staudinger, M. Luthy, *Helv. Chim. Acta* **1925**, 8, 65.
[4] W. F. Huebner, *Science (Washington, DC, U.S.)* **1987**, 237, 628.
[5] R. M. Minyaev, Y. A. Zhdanov, I. I. Zakharov, V. I. Minkin, *Vysokomol Soedin., Ser. B* **1974**, 16, 190.
[6] A. Novak, E. Whalley, *Trans. Faraday Soc.* **1959**, 55, 1484.
[7] M. L. Huggins, *J. Chem. Phys.* **1945**, 13, 37.
[8] G. Carazzolo, G. Putti, *Chim. Ind. (Milan)* **1963**, 45, 771.
[9] G. Carazzolo, *Gazz. Chim. Ital.* **1962**, 92, 1345.
[10] C. F. Hammer, T. A. Koch, J. F. Whitney, *J. Appl. Polym. Sci.* **1959**, 1, 169.
[11] J. Hengstenberg, *Ann. Phys. (Berlin)* **1927**, 389, 245.
[12] T. Uchida, H. Tadokoro, *J. Polym. Sci., Polym. Phys. Ed.* **1967**, 5, 63.
[13] G. Carazzolo, M. Mammi, *J. Polym. Sci., Part A* **1963**, 1, 965.
[14] C. R. Noe, C. Miculka, J. W. Bats, *Angew. Chem.* **1994**, 106, 1559; *Angew. Chem., Int. Ed.* **1994**, 33, 1476.
[15] J. W. Bats, C. Miculka, C. R. Noe, *Acta Crystallogr., Sect. C* **2007**, 63, o190.
[16] P. Deslongchamps, 'Stereo-electronic Effects in Organic Chemistry', Pergamon Press, Oxford–New York–Beijing–Frankfurt–Sao Paulo–Sydney–Tokyo–Toronto, 1984.
[17] A. Eschenmoser, M. Dobler, *Helv. Chim. Acta* **1992**, 75, 218.
[18] G. Quinkert, E. Egert, C. Griesinger, 'Aspekte der Organischen Chemie', Verlag Helvetica Chimica Acta and VCH, Weinheim–New York–Basel–Cambridge–Tokyo, 1995; G. Quinkert, E. Egert, C. Griesinger, 'Aspects of Organic Chemistry', Verlag Helvetica Chimica Acta and VCH, Weinheim–New York–Basel–Cambridge–Tokyo, 1996.
[19] C. R. Noe, M. Knollmueller, G. Goestl, B. Oberhauser, H. Voellenkle, *Angew. Chem.* **1987**, 99, 467; *Angew. Chem., Int. Ed.* **1987**, 26, 442.
[20] C. R. Noe, M. Knollmüller, E. Jangg, G. P. Gmeiner, *Chirality* **2007**, submitted.
[21] K. Mehraban, Ph.D. Thesis, Technische Universität Wien, Vienna, 1993.
[22] C. R. Noe, *Chem. Ber.* **1982**, 115, 1591.
[23] C. R. Noe, *Chem. Ber.* **1982**, 115, 1576.
[24] C. R. Noe, M. Knollmueller, K. Dugler, C. Miculka, *Chem. Ber.* **1994**, 127, 359.
[25] C. R. Noe, M. Knollmueller, C. Miculka, K. Dugler, E. Wagner, P. Etmayer, *Chem. Ber.* **1994**, 127, 887.
[26] C. R. Noe, M. Knollmueller, E. Wagner, H. Voellenkle, *Chem. Ber.* **1985**, 118, 1733.
[27] T. Bach, J. Lobel, *Synthesis* **2002**, 2521.
[28] C. R. Noe, M. Knollmueller, B. Oberhauser, G. Steinbauer, E. Wagner, *Chem. Ber.* **1986**, 119, 729.
[29] S. Winstein, B. K. Morse, *J. Am. Chem. Soc.* **1952**, 74, 1133.
[30] E. Dowty, ATOMS for Windows V6.3., a Program for Atomic-Structure Display, *Shape Software*, Kingsport, TN, 2006.
[31] Z. Otwinowski, W. Minor, in 'Methods in Enzymology 276', 'Macromolecular Crystallography, Part A', Eds. C. W. Carter Jr., and R. M. Sweet, Academic Press, 1997, pp. 307–326.
[32] G. M. Sheldrick, SHELXS-97, a Program for the Solution of Crystal Structures, Universität Göttingen, Göttingen, 1997.
[33] G. M. Sheldrick, SHELXL-97, a Program for Crystal Structure Refinement, Universität Göttingen, Göttingen, 1997.

Received September 3, 2007